

General Introduction

Life without light is unimaginable.

In these modern times artificial light allows us to extend our activities, such as working, travel and entertainment, beyond the daylight hours. Factories and office buildings are designed with no possibility of ever being adequately illuminated by daylight. Worldwide communication would be impossible if half the world could not dispel the darkness by turning on the light at the flick of a switch.

Turning on the light comes at a price. In fact, the biggest item of cost in producing light is the cost of electric power needed to operate the lamp. Worldwide about 20% of all electricity is used for lighting, making power efficiency one of the most important criteria for lamp design [1]. A second, almost as important, criterium is the aspect of colour rendering, which measures the ability of the light source to reproduce the colours of the illuminated object. The goal of colour rendering is to make the illuminated objects look as natural (i.e. as in daylight) as possible. A third important criterium in lamp design is the stability of the light source.

The search for a lamp that meets with all these criteria led to the the development of the high intensity discharge lamp (HID lamp). These are lamps that have high pressure (over 1 bar), small volume, high luminance and contain, in most cases, either mercury and/or sodium. A class of HID lamps are formed by the metal-halide lamps. These are high pressure mercury lamps containing one or more metal salts that produce a brilliant white light. They can display a power efficiency of nearly 40% which is quite staggering compared to the mere 4-6% of the incandescent lamp. This type of lamp seems to embrace all of the requirements mentioned above.

Unfortunately, the metal-halide lamp has certain issues that need to be dealt with such as instability, the need to operate the lamp in different orientations, and inhomogeneous colour. Complex transport phenomena result in non-uniformity of colours when the lamp is operated vertically. The lamp shows a bluish-white mercury discharge at the top of the lamp and a much brighter and whiter discharge from the additives at the bottom of the lamp [2]. Segregation of colours, or de-mixing, causes the illumination of an object to

result in strange colouring of the object, making the object look different than it really is. It also has a negative effect on the lamp's power efficacy. In order to improve these lamps the de-mixing phenomenon needs better understanding.

The research presented in this thesis aims at making a contribution to the ongoing process of understanding the fundamental processes going on in the metal-halide discharge lamp. This is expected to lead to an improvement of lamp design in terms of efficiency and colour rendering.

1.1 Gas Discharge lamps

Nearly all lamps that are used for general illuminating purposes are based on plasma technology. The exceptions are the highly inefficient incandescent (halogen) lamps and the relatively new LED's. The latter may, in the near future, prove to be a good alternative in some cases, especially as a replacement for incandescent and possibly fluorescent lamps. However, even if LED technology is advancing as rapidly as predicted, electrical discharges will have to supply the major share of light sources for at least another two decades [3] [4] [5]. In any case it is expected that the gas-discharge lamps are mostly qualified for the general illumination of large areas such as sports arenas, buildings and roads.

One of the major developments in the last century within the lamp industry is realized by the introduction of the gas discharge lamp. A unique advantage of the gas discharge lamp is the ability to select the atoms that radiate in the visible part of the spectrum. Combined with the fact that discharges radiate from regions with much higher temperature, a much higher efficiency can be reached than with the solid filament of the incandescent lamp. Another advantage of gas discharge lamps with respect to the incandescent lamp is that they can have a much longer lifetime.

The principle of a gas discharge lamp is based on the conversion of electric power into radiation by means of an electrical discharge in the gas medium in the lamp. In such lamps a weakly or moderately ionized plasma is created. A plasma is an ionized gas and consists of electrons, ions, neutrals and excited particles and is on average neutral. The gas is located, in general, in a discharge tube with two electrodes. [6]

The basic process that occurs in the discharge can be described as follows. The electrons are accelerated by an externally imposed electric field, their directed velocity will be scattered into random directions by elastic and inelastic collisions with heavy particles. The result of this ohmic heating is a high electron temperature. In the case of inelastic collisions, part the kinetic energy of the electrons is transformed into the internal energy of atoms. These inelastic collisions are essential for chemical processes, such as excitation, ionization and dissociation and the generation of radiation. The internal energy of the atoms is released as electromagnetic radiation as the atoms relax back to their lower energy states.

Generally, two groups of discharge lamps can be distinguished: low pressure and high pressure discharge lamps. Low pressure discharge lamps have a pressure of below 10^{-3} bar, are generally large in volume, low in luminance and power densities and the plasma

conditions in these lamps are far from equilibrium. High pressure discharge lamps generally have a small volume (a few mm³ or cm³), high pressure (more than 1 bar), high luminance, a large variety in power settings (10 W to 18 kW) while the plasma in these lamps are close to local thermal equilibrium (LTE). Due to their high intensity these lamps are often denoted by high intensity discharge (HID) lamps. [7]

Also, the energy transformation of the electrons, obtained from the electric field between the electrodes, into excitation, ionisation or dissociation of atoms or molecules and heat, is different in low-pressure and high-pressure discharge lamps. [7]

1.1.1 Low-pressure discharge lamps

In low pressure discharge lamps, the interaction frequency of electrons with heavy particles is low so that the electrons can attain a high temperature while the heavy particles, being in contact with the wall, remain relatively 'cool'. The most probable excitations are from the ground-state to the first excited states. These excited atoms emit resonance radiation. [7] The optimum pressure of metal vapour is around 1 Pa in low-pressure discharge lamps, but additionally a buffer gas with a high ionisation energy is added in order to contain the electrons and reduce the degradation of the electrodes.

In many cases mercury is the metal of choice since it has a high vapour pressure and can be easily excited. It generates light in the UV (254 nm and 185 nm), which can be converted into white visible light by phosphors, which is the case with the tubular fluorescent tube and its cousin the compact fluorescent lamp. Mercury is a highly efficient radiator, but half the photon energy is lost in the phosphor where a UV photon is converted into a visible one. Low pressure sodium lamps has a slightly lower efficiency, but the sodium resonant line at 590 nm coincides with the maximum sensitivity of the eye-sensitivity curve. Therefore no phosphors are needed, yielding a very efficient lamp, which unfortunately is monochromatic and thus of limited use. The application of the low pressure sodium lamp is restricted to road lighting, where colour distinction is considered to be less important [5].

In a low-pressure discharge lamp, the electron temperature is considerably higher than the heavy-particle temperature (temperature of atoms and ions). This is caused by the more effective energy gain of electrons compared to heavy particles in the discharge. The electric field accelerates ions and electrons, but the ions lose a substantial part of this kinetic energy at each elastic collision with another heavy particle due to the equal mass of the collision partners. The electrons lose only a very small percentage of their kinetic energy during elastic collisions with heavy particles due to the tremendous mass difference between electrons and heavy particles. Moreover, the electrons often excite atoms during inelastic collisions. If these excited atoms emit the energy as radiation, the kinetic energy of the atom does not increase, causing the heavy-particle temperature to stay low. [7]

1.1.2 High pressure discharge lamps

At a pressure higher than 1 bar the energy transformation process is different than for low pressure discharges. The mean free path of electrons decreases with increasing pressure,

which also increases the number of collisions. Although the electron passes only a small percentage of its kinetic energy to heavy particles during elastic collisions, the huge number of collisions ensures a considerable energy transfer from electrons to heavy particles. This results in an increasingly heavy-particle temperature with a simultaneously decreasing electron-temperature. In high pressure discharge lamps the electrons and heavy particles have temperatures between 1400 K and 8000 K. At these temperatures, the excitation of atoms is sufficiently high, resulting in radiation from transitions from excited states to the ground state and from excited states to other excited states. [7]

The resulting spectral power distribution of high-pressure discharge lamps consists therefore not only of resonance lines but also of spectral lines due to transitions between excited states. In fact, the resonance lines are even missing in high-pressure discharge lamps of sufficiently high pressure, because they are most probably reabsorbed in the outer regions of the plasma in the discharge tube. This is caused by the high density of metal atoms in high-pressure discharge lamps, which is even higher in the colder plasma regions. Since these atoms are mostly in the ground-state it is very likely that the absorption of resonance radiation takes place [7].

Typical high-pressure discharge lamps contain at least mercury or sodium. The advantage of sodium is, as with the low pressure discharge lamps, the wavelength of the resonance lines, which lie very close to the maximum of the sensitivity curve of the human eye. The advantages of mercury are the high vapour pressure, i.e. mercury is very volatile, and the high resistance of a mercury plasma due to the large cross-section for collisions between electrons and heavy particles. The latter makes it possible to operate the lamp on low currents and high voltages, which is desirable with respect to efficiency and also to low strain and long lifetime of the electrodes. The high pressure leads to large electric field strengths up to 600 V cm^{-1} . Thus high electrical power input into small discharge volumes is possible, which led to the development of the High Intensity Discharge (HID) lamp. [7]

Since the end of last century often metal-halide salts like TlI, NaI, DyI₃, HoI₃ etc are added to the mercury HID lamp in order to increase efficiency and colour properties. These lamps, containing both mercury and one or a combination of metal-halide salts, is called the metal-halide lamp.

1.2 The metal-halide lamp

In 1912 Charles Steinmetz was granted a patent [8] for a new light source. By adding small amounts of sodium, lithium, rubidium and potassium iodides he was able to modify the light output from 'an extremely disagreeable colour' to 'a soft, brilliant, white light'. It was not until much later, however, that a commercially viable lamp was produced along the same principles. In 1964 General Electric introduced a metal-halide lamp at the world trade fair in New York. [9]

Modern metal-halide lamps today operate under the same principles. They typically consist of a small burner about a centimeter in diameter and a centimeter or more in length surrounded by a larger protective outer bulb. The burner is made from poly-crystalline

alumina or quartz and is filled with noble gases, mercury (about 10 mg) and salt additives (a few milligram). Under operating conditions the mercury in the inner burner evaporates raising the pressure to several tens of bar. The advantages of metal-halide lamps remain much the same as in Steinmetz' original patent; they combine high luminous output across a broad spectrum of the visible range with good efficacy as compared to other light sources.

Despite all these advantages the growth in use of these lamps has been hampered by a number of limitations. For example the lamps can only be operated in a specified position e.g. vertically and when it can be operated in different orientations, the colour point is not the same. This non-uniform light-output reduces the design space for such lamps, and reduces its power efficiency. The lamp can become unstable which results in a disturbing flickering. It needs to cool down -the mercury vapour needs to condensate- before it can be re-ignited which is impractical in some cases. These limitations are caused by discharge physics, which is still relatively poorly understood. This section describes the principles of operation of metal-halide lamps, details the influence of the metal iodides and addresses the unwanted segregation of colours and how the study of these lamps under different gravity conditions can deepen our understanding of the complex transport phenomena and the overall energy balance of the lamp.

1.2.1 General principles of operation

The burner contains a rare gas for starting and a large quantity of mercury, acting as a buffer-gas, plus one or more of the additive metal-halides (usually iodides). In common with other HID lamps, the starting of metal-halide lamps has three distinct phases. First, the starting gas, usually a noble gas such as argon, is converted from a non-conductive to a conductive state. The inert gas is needed to start the lamp, because the vapour pressure of the mercury is too low at room temperature. The gas heats up the discharge tube to get the solid or liquid metal vaporised. This phase is rapidly followed by a period of anomalous glow discharge which heats the electrodes, producing the final phase of an arc discharge [6].

In operation, all of the mercury is vaporised, resulting in a high pressure, wall-stabilised arc at several bars of pressure. The additives also evaporate, additive molecules diffusing into the high temperature arc column, where they dissociate. The metal atoms are ionised and excited, giving off their characteristic myriad of spectral lines.

As metal atoms diffuse back to the walls, they encounter iodine atoms in the cooler gas near the walls and recombine to reform the iodide molecules. Because the average excitation potential of the metals (less than 4 eV) is much less than that of mercury (about 7.8 eV), the total power radiated in the added metal spectrum substantially exceeds that of the mercury spectrum, even though the mercury pressure is 100 times greater than the metal pressure. The spectrum, therefore, consists predominantly of the spectrum of the additives with the mercury spectrum superposed.

Because the additives show a considerable amount of lines distributed over the entire visible part of the spectrum, this in contrast to mercury whose spectrum contains almost no wavelengths longer than 579 nm, the metal-halide lamps have a vastly improved colour rendition over mercury lamps. Another advantage is the increase of luminous efficacy. For

a pure mercury arc only about 23 percent of the total radiation is in the visible part of the spectrum; in some of the iodide additives more than 50 percent of the total radiant energy can be visible. The net result is a lamp whose luminous efficacy can be over 120 lm/W whereas for mercury this is 55 lm/W. [1]

1.2.2 Influence of metal-halides in the discharge

Arc constriction

Unfortunately, additive metals may have an unwanted effect on the stability of the discharge. Metal additive atoms have many energy levels, a number of which are quite low-lying, so that the average excitation potential is quite low relative to the ionisation potential. This results in radiation loss near the flanks of the discharge, where most of the additive atoms are present, which then results in a contracted arc. This could give rise to constricted arc temperature profiles. Constricted arc profiles are poorly wall-stabilized. [10]

A wall-stabilized arc has a relatively steep temperature gradient at the wall. If the arc axis should move off centre toward one side, the temperature gradient on the other side would become less steep, resulting in less heat conduction loss, which would cause the temperature to rise in that region. The effect of the changes in the heat-conduction loss therefore partly cancel the initial motion of the arc column, thereby stabilising the arc against motion in the tube. [1]

However, the presence of sizeable quantities of metal additives in the arc can lead to constricted, poorly wall-stabilised arcs. A relatively large motion of the arc core in the tube causes little or no change in heat-conduction loss, and the walls exert no stabilizing influence on the arc. The arc position is therefore strongly affected by convection, turbulence, acoustic resonances, and (self-induced) magnetic forces. The arc of the lamp operated in vertical position can wander around periodically in the burner under the influence of convection currents, resulting in a flickering effect that is quite disturbing. The latter is also known as helical instability. Contraction of the arc is studied in various chapters of this thesis.

Arc broadening

Fortunately there are metals that can be added to the metal iodide arc that have exactly the opposite effect, they tend to broaden the arc. These are the alkali metal iodides: lithium, sodium, potassium, rubidium and cesium. The arc containing these species is wall-stabilized because of the larger diameter of the arc. [1]

The major effect of the alkali addition must be due to the low ionization potential of the alkali atom, which causes many more free electrons to be available in the low temperature region of the arc. The presence of these free electrons then allows for the electrical current flow, which leads to power dissipation and more heat generation in these low-temperature regions. This raises the temperature bringing about an increase in the diameter of the high temperature region of the arc and of the electrically conducting region. [1]

Radiation and absorption also influences the arc-broadening. Radiation emitted at the core is absorbed in the cooler outer regions of the discharge, adding to the energy to be dissipated as heat which causes the temperature to increase. Therefore, atoms with strong pressure-broadened resonance lines combining considerable absorption at the line core with considerable transport of energy in the line wings also have arc-broadening effects. For example, the addition of thallium iodide results in an increase in arc diameter because of radiation transport and absorption of the 377-nm thallium line [1]. Broadening of the arc is investigated in chapter 8.

The function of mercury in metal-halide lamps

It is not essential for the operation of the iodide cycle in a metal-halide lamp for mercury (Hg) to be present. However, there are several functions of mercury in the lamp mixture which are exceptionally useful.

1. Mercury makes it possible to achieve a high total pressure for operation while still having a low pressure at ignition, so that reasonable starting voltages can be obtained. Efficient operation of metal-halide lamps with a relatively high-pressure metal vapour requires a high total pressure filling to prevent rapid diffusion of dissociated metal and iodine atoms from the arc core to the tube wall. If dissociation took place primarily in the arc core and recombination took place primarily at the wall, the loss of energy due to the dissociation process would be very high, resulting in an inefficient lamp. [1]
2. An excess of mercury can react with excess iodine to form HgI_2 . If any free I_2 vapour is present in the lamp at ignition, starting voltages are very high. This is because the strong electron-attaching properties of I_2 interfere with the avalanche formation. The presence of mercury in excess then ensures that only HgI_2 is present at starting. Although HgI_2 is also an electron-attaching gas, its vapour pressure is substantially lower than that of I_2 and causes only a moderate increase in starting voltage. Another aspect of the HgI_2 is the effect on light emission. Excess iodine by itself tends to form I_2 near the walls and I_2 is strongly light absorbing. HgI_2 is relatively unstable and transparent. Excess iodine in the form of HgI_2 is as accessible as free iodine for preventing condensation of metals on the wall. [1]
3. Mercury has low thermal conductivity as opposed to alternatives such as zinc
4. Mercury causes the red flank of Na to broaden which results in a much better production of the colour red that is otherwise difficult to achieve.

1.2.3 Colour separation in the metal-halide arc lamps

Transport phenomena in metal-halide lamps: radial and axial segregation

A metal-halide lamp with colour separation has different colours along its axis. Figure 1.1(a) shows an example of colour separation in a lamp containing DyI_3 . Whereas the

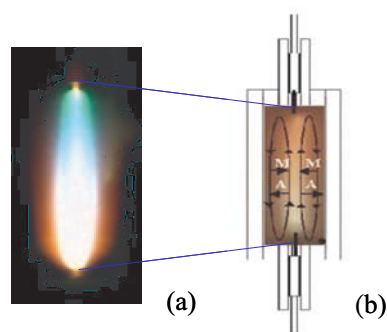


Figure 1.1: (a) Colour separation in an metal-halide lamp burner. The colours reproduced by the camera are not the actual colours, the top of the lamp is in fact bluish-white. (b) Schematic view of an metal-halide lamp; diffusion and convection of atoms (A) and molecules (M) are indicated by arrows.

bottom of the lamp is white with a reddish glow around it, the top is white-bluish. The cause is a complex interplay of diffusion and convection resulting in a non-homogeneous distribution of the radiating metals.

Let us concentrate on the radial direction and the role of diffusion. There are large temperature gradients across the radius of the lamp. Going from the wall at about 1200 K to the arc core at 6000 K metal-halide molecules will first dissociate and then ionize at the hot centre. The resultant density gradients cause strong diffusion fluxes, which are counteracted by the back-diffusion of other species: near the wall molecules diffuse inwards and atoms outwards, while near the centre atoms move inwards as the ions diffuse out. The diffusion speed of the molecules is significantly smaller than that of the atoms due to their size and mass difference. Ions and atoms have similar masses, but the ions at the centre diffuse faster due to ambipolar diffusion. In a steady state with equal in and outward fluxes, a lower speed is balanced by a higher partial pressure. The total effect is called radial segregation and results in a lowering of the partial metal pressure (in any chemical form) near the lamp centre [5].

In addition to diffusion, there is also convection in the lamp. In vertically operating lamps, convection causes an upward flow in the hot central arc region, which returns downwards along the cooler walls. The minority metal species follow the dominant mercury convection flow. However, radial segregation causes the metal, that rises in the centre and diffuses outwards to the wall, to be dragged downwards. The combined effect of convection and radial segregation is a decreased metal density in the upper part of the lamp, see figure 1.1 (b). Such axial segregation results in a non-homogeneous emission, called colour separation.

Depending on the competition with diffusion, the convection flow can have two opposite effects on the axial segregation. For relatively small convection flows we will find that an increase in convection will cause an increase of the axial segregation. On the other hand, in case of a high convection flow, we find that a further increase reduces the axial segregation

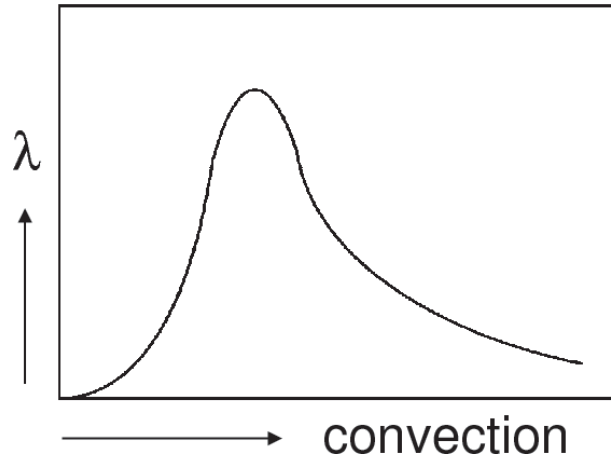


Figure 1.2: The Fischer curve [12] which represents the dependence of the axial segregation parameter λ on convection, or g .

as the species are better mixed in the lamp. By realizing that the convection is proportional to the total pressure it can be understood that there is one pressure for which the axial segregation reaches a maximum, see figure 1.2. Fischer characterized axial segregation with a segregation parameter λ such that [12]

$$p_{\{\alpha\}}(z) = p_{\{\alpha\}}(0) \exp(-\lambda_{\{\alpha\}}z), \quad (1.1)$$

where z is the axial position relative to the tip of the lower electrode and $\lambda_{\{\alpha\}}$ is called the segregation parameter for the element α .

Elemental density and elemental pressure

Elemental density is defined as the density that contains all molecular, atomic and ionic contributions of a particular element. For example, for element α (denoted with $\{\}$), the number density of a particular element n_{α} is the sum over all species containing that element,

$$n_{\{\alpha\}} = \sum_i R_{i\alpha} n_i \quad (1.2)$$

The stoichiometric coefficient $R_{i\alpha}$ counts the number of α -nuclei in the compound or species i . For example for DyI_3 the elemental density of Dy ($\alpha = \text{Dy}$) in a lamp containing DyI_3 can be described as

$$n_{\{\text{Dy}\}} = [\text{Dy}] + [\text{Dy}^+] + [\text{DyI}] + [\text{DyI}_2] + [\text{DyI}_3] + 2[\text{Dy}_2\text{I}_6] + 3[\text{Dy}_3\text{I}_9] + \dots \quad (1.3)$$

The stoichiometric coefficient of DyI_3 equals for Dy $R_{i\alpha}=1$, while for I $R_{i\alpha}=3$ for the molecule DyI_3 . The summation of equation 1.2 runs over all species. In an analogue way we can determine elemental pressure $p_{\alpha}=n_{\alpha}kT$, for Dy the elemental pressure $p_{\{\text{Dy}\}}=n_{\{\text{Dy}\}}kT$. Elemental densities are shown in chapter 6.

Gravity and segregation

Above we have seen that the axial segregation is caused by the combination of convection and diffusion. The convection is the result of gravity and thus directly related to the value of the free fall acceleration $g = 9.8 \text{ m/s}^2$. By varying the acceleration of the lamp the gravity conditions can be varied, making it possible to separate the role of either diffusion or convection in the segregation phenomenon. It is possible to create two extreme situations by varying the gravity conditions.

1. No convection. Under micro-gravity conditions, the convection velocity is very small so that diffusion is dominant. On top of the density decrease caused by the temperature, we are still able to observe radial de-mixing; i.e. the concentration of the radiating species will still be lower in the centre of the lamp as compared to the regions near the wall.

2. High convection. Under hyper-gravity conditions, the convection velocity increases so that the concentration of the additives in the lamp becomes well mixed; any radial de-mixing caused by diffusion will be eradicated by convection. This can be achieved by placing the lamp under high acceleration conditions.

Both micro- and hyper-gravity conditions were realized during parabolic free falls in an Airbus airplane of the European Space Agency (ESA). There the gravity varied between 0- g and 2- g . The lamps were designed such that de-mixing is at a maximum at 1- g . These experiments revealed that at both 0- g and 2- g de-mixing was dramatically reduced. However, the period (almost 20 s) of zero- g during parabolic flights is too short to stabilize the plasma.

It is therefore that the experiments were repeated at the international space station ISS where micro-gravity is sustained. The experiments were done in the week of April 24th, 2004 by the Dutch astronaut André Kuipers. The results of these experiments are shown in chapter 3. In order to create an environment of prolonged hyper-gravity and to enhance the dynamical range of the experiments to higher gravity values, a centrifuge was built that accelerates from 1 to 10 g . The results of these experiments are presented in chapter 4.

Experiment and model

It is currently beyond our capabilities to fully understand and model a commercial metal-halide lamp with complex shape and chemistry [12]. Therefore, the measurements have been performed on a reference lamp with simple geometry and chemistry. The absence of convection under micro-gravity conditions greatly simplifies the problem. The measurements reveal a great deal about lamp behaviour, which needs to be reproduced by any valid lamp model. Qualitatively the lamp behaviour is well understood and the measurements supply ample data for quantitative model validation. A comparison between experiment and model is presented and discussed in chapter 5. Obviously, changing gravity is not a practical solution, but it helps to identify how to optimize discharge parameters, so we can illuminate our world using less energy.

A simple model based on an assumed parabolic temperature profile and long aspect

ratios was published in [12]. More advanced models have since been made [15] [16]. A numerical model was constructed by Beks [14] that uses less assumptions on the nature of the discharge, calculating more of the lamp properties from first principles than earlier models. This model should calculate all essential properties self-consistently. This involves, amongst others, calculating the convection and diffusion of species throughout the discharge region, calculating the emission and absorption of light and accurately describing the energy balance in the lamp. To build this model we have at our disposal the plasma simulation package Plasimo [17] [18] developed at the Eindhoven University of Technology by a succession of graduate students and researchers over the past 15 years.

1.3 Scope of Thesis

The work presented in this thesis is aimed at obtaining a better understanding of the segregation phenomena in metal-halide lamps by means of experimental investigation. This PhD project is part of a larger project for the understanding of the energy balance of metal-halide lamps and the plasma transport processes that are responsible for segregation phenomena in these lamps. Qualitatively the mechanism is understood, but quantitatively the disagreement between theoretical models and experiment is often large. Therefore more in-depth studies are needed and quantitative data from experiments are required to validate models. The final goal is to set up a complete theoretical model to fully understand the energy balance and transport processes in such chemically complex plasmas. This grand model can then be used to design lamps with high efficiency and good colour rendering. The primary objective of this project is to use poly-diagnostic tools in order to study the plasma properties such as the density of species and temperature in the metal-halide lamp.

Metal-halide lamps contain a chemically complex discharge. The spectrum of such a discharge contains a myriad of lines. We have used Optical Emission Spectroscopy (OES) to analyse these lines which yielded, after calibration and inversion, the radially resolved atomic state distribution function (ASDF). The ASDF yields a wealth of information regarding the species distribution and temperature. It is assumed by most researchers that the discharge in these lamps are in local thermodynamic equilibrium (LTE). This implies that only one temperature field is needed to describe all the processes. However the important question remains whether this LTE assumption is valid or not. If LTE is not established, this would imply that the local chemical composition, the radiation generation and transport processes are determined by a multitude of temperatures. This would make the description of the system very complex. The validation of the LTE assumption requires different temperature measurements. The ASDF can give insight about a possible departure from LTE.

It is known from theory that segregation, which is governed by the competition between diffusion and convection, is strongly influenced by convection, and therefore gravity. It is therefore of great interest to study the lamp under various gravity conditions ranging from micro-gravity to hyper-gravity. At micro-gravity diffusion of species can be exclusively studied as there is no convection. At hyper-gravity convection dominates the transport of

species in the lamp. Previously the lamp was studied under the micro-gravity conditions of the space shuttle [19] [20] and under micro to hyper-gravity during parabolic flights [21]. The former experiments yielded no information regarding the density or temperature distribution, the latter did not have sustained gravity conditions for more than 20s, which is not enough to stabilize the arc.

In the research described in this thesis we used the gravity-free environment of the international space station ISS for the micro-gravity experiments and a centrifuge that imposes hyper-gravity of up to 10 g on the lamp. We have used optical emission spectroscopy to study segregation under these varying gravity conditions. The experiments yielded the major plasma parameters such as species distribution and temperature.

The absence of convection under micro-gravity conditions greatly simplifies the problem. The measurements reveal a great deal about lamp behaviour, which needs to be reproduced by any valid lamp model. Qualitatively the lamp behaviour is well understood and the measurements supply ample data for quantitative model validation. Modelling investigations were performed by Beks [14]; results of the comparison between experiment and model are included in this thesis.

It is of interest to study the discharge with x-ray techniques that allow for measurements anywhere in the lamp, in contrast to optical methods which are limited to the core or regions close to the core. Two types of x-ray technique were used: x-ray induced fluorescence (XRF) and x-ray absorption spectroscopy (XRA).

An extensive quantitative study of the arc constituents was done by means of x-ray induced fluorescence (XRF). Synchrotron radiation from the Advanced Photon Source of the Argonne National Laboratory was used to excite fluorescence of the various species of the discharge, allowing for the direct measurement of the elemental densities, some of which are optically inaccessible.

The primary observable of the XRA is the Hg density distribution, which by means of the ideal gas law $p = nkT$ can be translated into a heavy-particle temperature distribution (assuming isobaric conditions). XRA has very high spatial resolution which is very important in these lamps because of the fact that the discharge has a very steep temperature gradient. The comparison of the gas temperature with the electron (excitation) temperature as deduced from OES measurements gives insight in potential deviations from LTE.

1.4 Thesis outline

In order to obtain a large amount of data that can be used for both model validation and cross-comparison among the individual experiments, a poly-diagnostic approach was chosen for the lamp experiments.

OES is performed on lamps under normal- micro- and hyper-gravity conditions. Also a comparison is made between the modelling investigations done by Beks [14] and the micro-gravity results. The lamp is also investigated using x-ray techniques that can penetrate all parts of the lamp, namely XRF and XRA. XRF was used to measure the spatial

distributions of the arc constituents. XRA was used to determine the temperature profile. Lamps containing different types of lamp filling are also studied by XRA.

Chapter 2 deals with OES at normal-gravity. Here the spectrum of the metal-halide lamp in question is introduced and after intensity calibration and radial transformation the ASDF, which provides the density distribution of the atoms, ions and electrons of Dy and Hg, is constructed. A comparison is made between different data-sets for the transition probabilities. The validity of LTE is briefly investigated.

Chapter 3 deals with the study of segregation at micro-gravity. It is clear that no axial and only radial segregation exists in a micro-gravity environment. Density distributions of atoms and ions at different powers are shown, together with temperature profiles. A comparison is made between the measurements done at normal and micro-gravity. For this purpose temperature profiles, intensity and concentration profiles are compared at different lamp powers.

Chapter 4 is a follow up of the micro-gravity experiments and deals with hyper-gravity. The lamp and OES setup are placed in a rotating gondola. The resultant gravity can be varied continuously from 1 to 10 g. The result of the increased gravitational acceleration is an enhanced convection flow within the lamp. Webcam images are presented that clearly show the behaviour of the discharge at increased gravity. Line-of-sight intensity profiles are used to investigate the effects of the increase in gravity. The results are used to recreate the curve produced by the theoretical model of Fischer.

The results of the micro-gravity experiments from chapter 3 are compared with modelling investigations of Beks [14]. The density and temperature profiles together with the concentration profiles are compared. This can be found in chapter 5.

Chapter 6 shows the results from the XRF measurements of the arc constituents Hg, Dy and I. A simplified theoretical description of radial fluxes is presented and is used for the comparison between the OES and the XRF results.

Chapter 7 shows temperature profiles measured with XRA with an improved data analysis that shows dramatically different results from experiments reported previously by Zhu [13]. Comparisons are made between the temperature distribution obtained with OES and XRA.

Lamps with different fillings which include NaI, TII, Dy₃ and a commercial lamp containing a combination of these are measured with XRA and presented and discussed in chapter 8.

1.5 The lamps

Because of the need to simplify the complex commercial metal-halide lamp for the experiment and model, almost all the measurements have been performed on a reference lamp [22] with a simple geometry and chemistry, see figure 1.3. Table 1.1 shows the various lamps and lamp geometries and the various experiments that used them. All burners were made of quartz except for the XRA experiments in chapter 8 (XRA II), here PCA burners were used, see figure 1.4.



Figure 1.3: A COST reference lamp [22] used for most experiments in this thesis. The burner is made of quartz



Figure 1.4: One of the lamps used for the XRA experiments. This type of lamp has either quartz COST burners (as in chapter 7) or PCA burners (as in chapter 8 and depicted here). The outer bulb geometry for both chapter 7 and 8 is the same.

Experiment	D_{in}	D_{out}	L_{arc}	m_{Hg}	salt	power	chapter
OES normal- <i>g</i>	8	20	18	10	DyI ₃	100	2
OES micro- <i>g</i>	8	20	18	10	DyI ₃	70-150	3,5
OES micro- <i>g</i>	8	20	18	10	-	70-150	3,5
OES hyper- <i>g</i>	8	20	18	5, 7.5, 10	DyI ₃	130	4
OES hyper- <i>g</i>	4	20	20	0.75, 2.5	DyI ₃	130	4
XRF	8	20	18	10	DyI ₃	145	6
XRA I	8	120	18	10	DyI ₃	145	7
XRA I	8	120	18	10	-	145	7
XRA II	8	120	18	10	DyI ₃ , TII, NaI, mix	70	8

Table 1.1: Lamps used for this study. The diameters D_{in} and D_{out} are inner and outer diameter and are given in mm. The arc length L_{arc} is also given in mm. The power is given in W and the Hg mass in mg. Wall thickness of both burner and jacket is 1 mm, except for the PCA burners in chapter 8 that have a thickness of 0.55 mm. All lamp burners are shaped as cylinders.

Bibliography

- [1] J. Waymouth, *Electric discharge lamps*, MIT press, Cambridge, 1971
- [2] Zollweg R J, 1975 IES J. **4** 12-18
- [3] Solid-State Lighting Research and Development Portfolio, Navigant Consulting, 2006
- [4] M. Krames, *Progress in High power light-emitting diodes for solid state lighting*, Proc. 11th Int. Symp on the Science and Technol. of Light Sources, May 2007, Shanghai, ed. M.Q. Liu and R. Devonshire, p571-573
- [5] Stoffels W W, Nimalasuriya T, Flikweert A J, Mulders H C J, 2008 Plasma physics and controlled fusion, special issue, invited papers from the 34th european physical society conference on plasma physics, Warsaw, Poland, 2-6 July 2007, accepted for publication.
- [6] Coaton J R, Marsden A M, *Lamps and Lighting*, Arnold, London, 4th edition, 1997
- [7] Flesch P, *Light and light sources High intensity discharge lamps*, Springer-verlag, Berlin Heidelberg, 2006
- [8] Steinmetz C P, *Means for producing light* , U.S. Patent 1 025 932, 1902.
- [9] Beks M L, van Dijk J, Hartgers A, van der Mullen J J A M, IEEE *accepted for publication*
- [10] Elenbaas W 1951 *The high pressure mercury vapour discharge*, 1st ed., (North-Holland publishing company)
- [11] Fischer E 1978 *Influences of External and Self-Magnetic Fields on the behaviour of discharge lamps*, Philips GmbH Forschungslaboratorium Aachen Lobornotiz nr 13/78.
- [12] Fischer E, 1976 J. Appl Phys. **47** 2954
- [13] X. Zhu *Active spectroscopy of metal-halide lamps* PhD Thesis Eindhoven University of Technology (2005)
- [14] Beks M L, Hartgers A, van der Mullen J J A M, 2006 JPhysD **39** 4407
- [15] Dakin J T *et al* 1989 J. Appl. Phys. **66** 4074
- [16] Hashiguchi S, Hatase K, Mori S and Tachibana K 2002 J. Appl Phys. **92** 45
- [17] Benoy D A, 1993 *Modelling of Thermal Argon Plasmas* PhD Thesis Eindhoven University of Technology, the Netherlands
- [18] van Dijk J 2001 *Modelling of plasma light sources* PhD Thesis Eindhoven University of Technology, the Netherlands

- [19] Bellows A H, Feuersanger A E, Rogoff G L, and Rothwell H L, 'HID convection studies: a space shuttle experiment,' 1984 Illuminating Engineering Soc. Meeting
- [20] Bellows A H, Feuersanger A E, Rogoff G L, and Rothwell H L, 'Convection and Additive segregation in High pressure lamp arcs: Early results from a space shuttle experiment,' 1984 Gaseous electronics Conf., 1985 Bull. Amer. Phys. Soc. Vol **30**, p 141
- [21] Flikweert A J, van Kemenade M, Nimalasuriya T, Haverlag M, Kroesen G M W and Stoffels WW 2006 J.Phys.D **39**, 1599
- [22] Stoffels W W, Flikweert A J, Nimalasuriya T, van der Mullen J J A M, Kroesen G M W, Haverlag M, 2006 Pure Appl. Chem. **78** No 6
- [23] J.A.M. van der Mullen, Phys. Rep. **191** 109 (1990)
- [24] Curry J J, Sakai M and Lawler J E 1998 J. Appl. Phys. **84**, 3066
- [25] Lister G G, Lawler J E, Lapatovich W P and Godyak V A 2004 Rev. Mod. Phys. **76**, 541
- [26] Stoffels W W, Haverlag M, Kemps P C M, Beckers J and Kroesen G M W 2005 Appl. Phys. Lett. **87** 1
- [27] Mitchner M and Kruger Jr C H 1973 *Partially ionized gases* ,1st ed., (John Wiley and Sons).
- [28] Flikweert A J, Nimalasuriya T, Stoffels W W, Kroesen G M W 2007, PSST **16** 606